Materials Science and Engineering A 539 (2012) 68–73

Contents lists available at SciVerse ScienceDirect

Materials Science and Engineering A

journal homepage: www.elsevier.com/locate/msea

Formation of multiple twins and their strengthening effect in nanocrystalline Cu/Zr multilayer films

J.J. Niu[a], P. Zhang[a], R.H. Wang[b], J.Y. Zhang[a], G. Liu[a,*], G.J. Zhang[b], J. Sun[a,b,**]

[a] State Key Laboratory for Mechanical Behavior of Materials, Xi'an Jiaotong University, Xi'an, 710049, China
[b] School of Materials Science and Engineering, Xi'an University of Technology, Xi'an, 710048, China

ARTICLE INFO

Article history:
Received 4 August 2011
Received in revised form
13 December 2011
Accepted 11 January 2012
Available online 20 January 2012

Keywords:
Multilayer films
Multiple twins
Formation mechanism
Strengthening effect

ABSTRACT

Multiple twins are experimentally observed within Cu grains in nanostructured Cu/Zr multilayer films. Formation of the multiple twins occurs through the sequential emission of partial dislocations not only from the grain boundaries but also from the Cu/Zr interfaces, which are driven by extremely high internal stresses and highly complex stress state caused by the inhomogeneous microstructures. The multilayers with multiple twins exhibit hardness higher than those with single or coplanar twins, indicative of a significant strengthening effect of the multiple twins.

1. Introduction

Recently, nanocrystalline face-centered cubic (fcc) metals with a high density of nano-sized twins have been of great interest because of their excellent mechanical properties, such as high strength and high ductility [1–3]. The significant strengthening effect of twins is owing to the unique dislocation–twin boundary interaction [4,5], and the strengthening response is closely dependent on the density or the thickness of the twins [3,6]. In nanostructured thin films, the hardness was also found to increase monotonically with increasing volume fraction of twined grains [7]. The twins used for studying their strengthening effect in nanocrystalline fcc metals are usually coplanar or single twins [1,6,7]. For example, the twins in sputtered Cu and stainless-steel films are preferentially oriented perpendicular to growth direction [8] and the twins within a same grain are parallel in electrodeposited Cu [6]. Multiple twins, where two or more twins meet in a confined area, have been frequently observed [9–14] in nanocrystalline fcc metals that are prepared by severe plastic deformation techniques. But the separated effect of multiple twins on strength is hard to determine, because the severe plastic deformation will simultaneously cause remarkable refinement in grain size and noticeable increase in dislocation density, which makes the strengthening effects interrelated and complicated. How can the multiple twins contribute to the strength is far from clear, neither quantitatively nor qualitatively.

In this paper, we demonstrate that abundant multiple twins are formed within the Cu grains in nanostructured Cu/Zr multilayer films even under no external stress. It is conformed that the formation occurs through the sequential emission of partial dislocations from not only the grain boundaries but also the Cu/Zr interfaces, which are driven by the extremely high lattice mismatch stress and highly complex stress state caused by the inhomogeneous microstructures. Typically, the high lattice mismatch stress and highly complex stress state are two characteristics of nanocrystalline multilayer films (NMFs). The multilayer films with multiple twins exhibited hardness higher than those with single or coplanar twins, indicative of a significant strengthening effect of the multiple twins. Traditional strengthening models for NMFs mainly cover the influences of constituent phases, modulation period (λ), and modulation ratio (η). Our results presented in this paper show that the effect of twins, especially multiple twins, should be taken into account in quantitatively describing the strength/hardness of NMFs, which may be useful for the development of advanced nanostructured materials.

2. Experimental procedure

Cu/Zr NMFs with total thickness of 1 μm, were deposited on oxidized Si substrate by using direct current (DC) magnetron sputtering method at room temperature. To get better adhesion

* Corresponding author. Tel.: +86 29 82668610; fax: +86 29 82663453.
** Corresponding author.
E-mail addresses: lgsammer@mail.xjtu.edu.cn (G. Liu), junsun@mail.xjtu.edu.cn (J. Sun).

0921-5093/$ – see front matter © 2012 Elsevier B.V. All rights reserved.
doi:10.1016/j.msea.2012.01.046

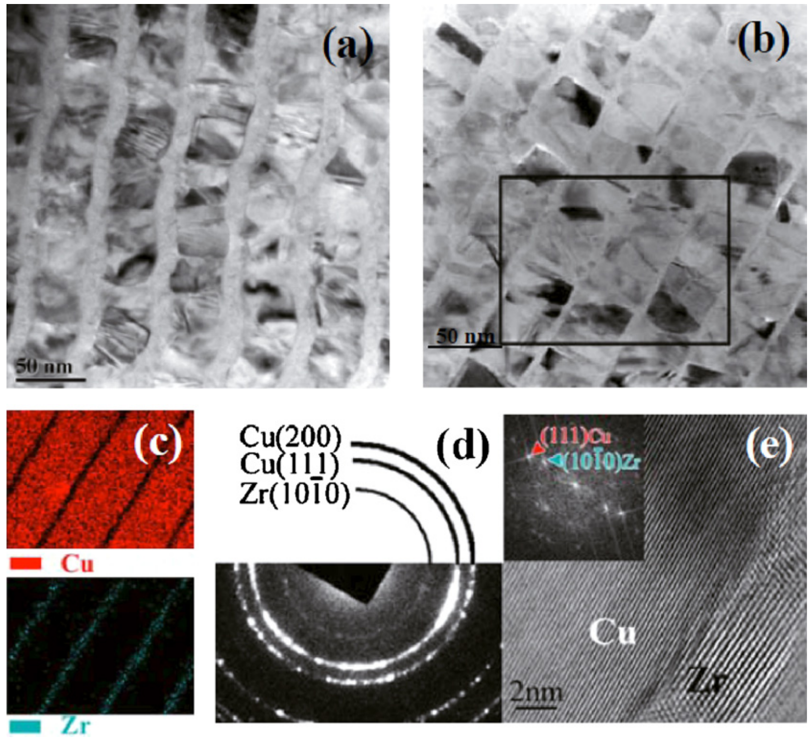

Fig. 1. Representative TEM image of Cu/Zr NMFs with $\eta = 2$ (a) and $\eta = 9$ (b); (c) is the Cu and Zr composition mapping corresponding to the marked area in (b); (d) the corresponding selected area diffraction patterns (SADP); (e) HRTEM image showing the crystalline Cu and Zr phases and the Cu/Zr interface.

between the film and the substrate, the Zr layer was first deposited onto the substrate and finally the top layer of the multilayer was Cu. Modulation period was kept constant as $\lambda = 50$ nm, while two modulation ratios, *i.e.*, $\eta = 9$ and 2 (η defined as the ratio between Cu layer thickness and Zr layer thickness) were prepared. The deposited multilayer films were subsequently annealed at 150 °C for 1 h in a high vacuum environment (less than 10^{-8} mbar) to stabilize the microstructure. The residual stress of NMFs was determined by using X-ray diffraction (XRD) and the traditional “sin 2ψ method”. This method is based on the measurement of the shift of a diffraction peak position recorded for different ψ angles [15,16]. In this approach, the strain $\varepsilon_{\varphi\psi}$ is defined as the difference in the d spacing for stress free and stressed lattice, as given in Eq. (1). This strain was measured along laboratory co-ordinate axis, perpendicular to a particular ($h\,k\,l$) plane used in the coordinate axes and expressed in terms of stress after assuming that the film is isotropic and the stress state is biaxial, and inserting Hook’s law. The resultant equation takes a simple form of Eq. (1) and residual stress in the film is calculated using

$$\varepsilon_{\varphi\psi} = \frac{d_{\varphi\psi} - d_0}{d_0} = \frac{1+\nu}{E}\sigma_\varphi \sin^2\psi - \frac{\nu}{E}(\sigma_{11} + \sigma_{22}), \tag{1}$$

where $d_{\varphi\psi}$ is the lattice spacing of ($h\,k\,l$) planes titled by ψ and rotated by φ within the plane of the film with respect to axes σ_{11}, and d_0 is the strain free lattice spacing. The terms E, ν, and σ_φ are the elastic constant, Poisson ratio, and normal stress in the direction φ, respectively. From the plot of $d_{\varphi\psi}$ *vs.* $\sin^2\psi$, the residual tress in the Cu layer (σ_r^{Cu}) and Zr layer (σ_r^{Zr}) can be respectively calculated from the slope of the line. Data was taken at ten different ψ tilts for getting accurate d spacing shift. The total residual stress of the NMFs, σ_r, is finally determined by simply averaging on the two constituent layers as

$$\sigma_r = \frac{t_{Cu}\sigma_r^{Cu} + t_{Zr}\sigma_r^{Zr}}{t_{Cu} + t_{Zr}}, \tag{2}$$

where t_{Cu} and t_{Zr} are the thickness of the Cu layer and Zr layer, respectively. The residual stresses were determined about 230 ± 80 MPa for all the annealed Cu/Zr NMFs, which is far lower than their yield strength. Transmission electron microscopy (TEM) experiments were performed on a JEOL-2100F, operating at 200 kV to observe the grain structure and the interface. The in-plane grain size of the Cu layer were measured using quantitative bright-field TEM images. Due to contrast variations in delineating the grain boundaries, some inaccuracies were introduced.

The hardness of multilayers was measured at room temperature by instructed nanoindentation experiments, which was performed by using Fischerscope HM2000XYp indenter with a Vickers indenter tip (Triboindenter, Hysitron, Minneapolis,MN). The load was increased to maximum loads for 5 s, held for 2 s, and then unloaded for 5 s. The maximum load was kept below a contact depth of 200 nm to avoid the substrate effect. Before every testing, drift monitor/correction was performed. Nine indents were made on each sample with an inter-indent spacing of 8 μm.

3. Results and discussion

3.1. Microstructure

Cross-sectional TEM images are displayed in Fig. 1(a and b), respectively, for the Cu/Zr NMFs with $\eta = 2$ and 9, clearly showing alternate layers. Composition mapping in Fig. 1(c) corresponding to the square area in Fig. 1(b) shows the two phases of Cu and Zr. Single layer of grains are found in every Cu layer, which means the out-of-plane size of the Cu grains is equal to the thickness of the Cu layer. The average in-plane grain size of the Cu layer was determined, as presented in Table 1. Selected area diffraction patterns (SADP) reveal a main ⟨1 1 1⟩ out-of-plane orientation for the Cu layer and a ⟨1 0 $\bar{1}$ 0⟩ for the Zr layer (Fig. 1(d)). The high resolution TEM image (Fig. 1(e)) shows a sharp interface between the Cu and Zr layers. Fig. 2 shows the planar TEM images of the Cu grains

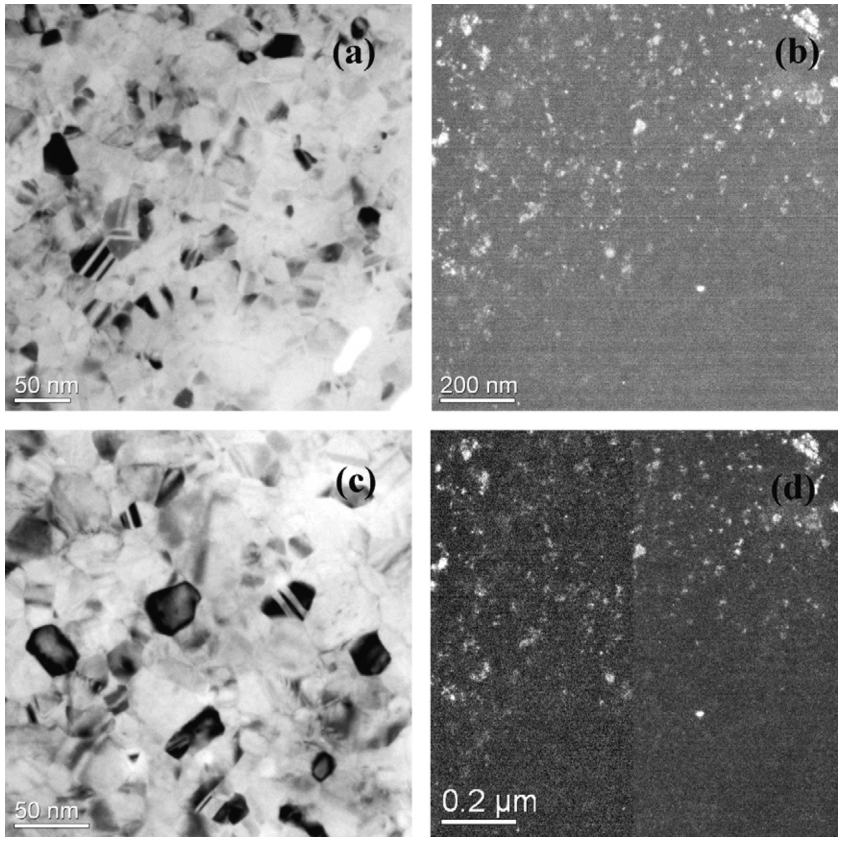

Fig. 2. Representative planar TEM images of the Cu grains ((a and c)) and Zr grains ((b and d)) in the $\eta = 2$ ((a and b)) and 9 ((c and d)) Cu/Zr NMFs, respectively. Note that the Zr layer is very thin and so it is very hard to obtain the planar TEM image of the single Zr layer without the Cu layer. Dark field TEM images are therefore taken to select the Zr grains in (b and d).

((a and c)) and Zr grains ((b and d)) in the $\eta = 2$ ((a and b)) and 9 ((c and d)) Cu/Zr NMFs, respectively. Note that the Zr layer is very thin and so it is very hard to obtain the planar TEM image of the single Zr layer without the Cu layer. Dark field TEM images are therefore taken to select the Zr grains in Fig. 2(b and d).

Careful microstructural observations revealed that abundant twins were existed within the Cu grains in both the two NMFs. Statistical results based on examination of above 800 grains show only a sight difference in the percentage of twined Cu grains (f_t: the ratio between the number of Cu grains with twins and the number of all countered Cu grains) between the two NMFs, as presented in Table 1. However, the twins in $\eta = 2$ multilayers are predominantly single twins, while most of the twined Cu grains in $\eta = 9$ multilayers contain multiple twins. See Table 1, the percentage of Cu grains with multiple twins, f_{mt}, is as high as 50% in the $\eta = 9$ multilayers. Multiple twins, including three-fold, four-fold and five-fold twins, are clearly visible. A typical five-fold twin is shown in Fig. 3. Fig. 3(a) is a low magnification cross-section TEM image to show the position of the five-fold twin as marked by white lines. Fig. 3(b) is a magnified image of the five-fold twin, where the five twin boundaries are labeled TB1-TB5 in anticlockwise order. The corresponding fast Fourier transformation (FFT) and inverse FFT image of the five-fold twin is shown in Fig. 3(c and d), respectively. Generally, the ideal twin angle of 70.5° would leave a gap of about 7.4° when closing the 360° to form five-fold twin [17]. In present five-fold twin, as typically shown in Fig. 3(b), all of the angles between TBs are larger than 70.5°. But the deviation between the maximum and minimum angle is only 2°, indicating that the 7.4° gap is evenly shared by the five twins. This gap is accommodated by the elastic strain originating from the lattice mismatch stress, which will be discussed later.

Table 1
Summary of the microstructural parameters and hardness.

Multilayer	h_{Cu} (nm)	d_{Cu} (nm)	f_t (%)	f_{mt} (%)	H (GPa)
Cu/Zr ($\eta = 2$)	33.3	43 ± 4	70 ± 5	11 ± 3	4.90 ± 0.1
Cu/Zr ($\eta = 9$)	45.0	45 ± 5	72 ± 3	52 ± 8	5.45 ± 0.1

3.2. Formation of multiple twins

Zhu et al. [17] proposed that the five-fold twins in nanocrystalline fcc metals are formed *via* sequential twining through the emission of Shockley partials from the grain boundaries or twin boundaries. According to this mechanism, the five-fold twins are evolved from two-fold, three-fold and four-fold twins step by step. It is expected that some intermediate three- and four-fold twins will be coexistent with the five-fold twins. In present NMFs, abundant three- and four-fold twins were observed besides the five-fold twins. Fig. 4(a) typically shows a four-fold twin within another Cu grain. This confirms the formation mechanism of sequential partial emission to some extent. Compared with previous reports on multiple twins [9,17–20], a distinct finding in the NMFs is that the partials can be also emitted from Cu/Zr interfaces. The interfaces promote and mediate the formation of multiple twins in NMFs. One can find that the twin boundaries TB2, TB4 and TB5 in Fig. 3(b) are from the Cu/Zr interface, while the twin boundaries TB1 and TB3 from the grain boundaries.

Two critical requirements have been derived from the sequential twining mechanism: high stress and variation in stress orientation [17]. The high stress is needed to emit Shockley partials, while the variation in stress orientation is to ensure the emission

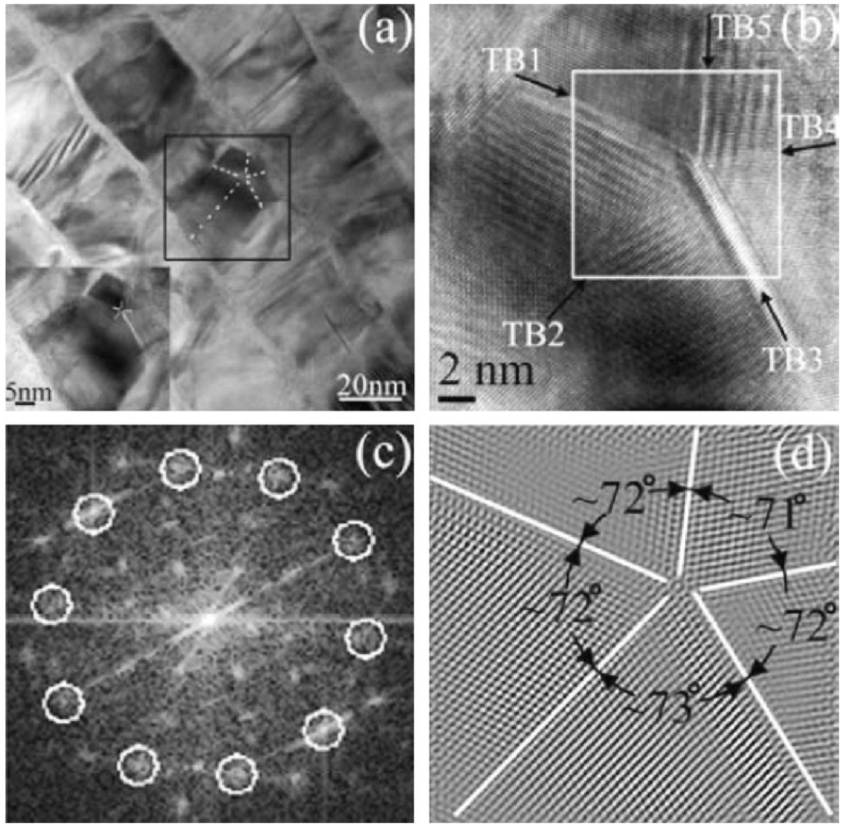

Fig. 3. (a) Overview of a five-fold twin in the η = 9 NMFs; (b) magnified TEM image of the five-fold twin; (c and d) are the fast Fourier transformation image and inverse fast Fourier transformation of the five-fold twin, respectively. The twin boundaries of TB2, TB4, and TB5 are from Cu/Zr interfaces, while TB1 and TB3 from Cu grain boundaries.

of partials from different orientations. Severe plastic deformation techniques, such as ball milling [21] and high-press torsion [11,12,18], involve high external stress and complex stress states, meeting the requirements for forming five-fold twins. Besides the high external stress, atomic simulations have found that local internal stress at the grain boundaries of nanocrystalline fcc metals can reach several GPa [20], sufficient to initiate Shockley partials even with no external stress. Annealing treatment is required to relax the internal stress and to trigger the emission of partial dislocations. In present Cu/Zr NMFs, the driving force for forming five-fold and multiple twins is come from the high internal stress, in particular the lattice mismatch stress between the two constituent layers. A lattice mismatch of $\varepsilon_{\text{mis}} \sim -5.6\%$ can be estimated [22] in the Cu layer. This lattice mismatch corresponds to a compressive interface mismatch stress of above 10 GPa ($\sigma_{\text{mis}} = Y_{\text{Cu}}\varepsilon_{\text{mis}}$ with $Y_{\text{Cu}} \sim 190$ GPa [23] being the biaxial modulus of Cu). While the critical stress σ_c to nucleate Shockley partials is estimated about 2.5 GPa by using Chen et al.'s expression [24]

$$\sigma_c = M\left(\frac{2\alpha G b_p}{D_{\text{Cu}}} + \frac{\gamma_{\text{sf}}}{b_p}\right), \tag{3}$$

where α is a parameter reflecting the character of the dislocation (=1.0), G is shear modulus of the Cu (48 GPa), γ_{sf} (78 mJ/m^2) is the stacking fault energy, b_p (0.148 nm) the magnitude of Burgers vectors of the partial dislocations, and M (~3.1) the Schmid factor [25]. Obviously, the interface mismatch stress is much larger than σ_c. During annealing treatment, Shockley partials will be favorably emitted from the Cu/Zr interfaces to relax the extremely high interface mismatch stress. Moreover, the present Cu/Zr NMFs have inhomogeneous microstructure, which is characterized by the interfaces and grain boundaries surrounding the Cu grains. This makes the internal stress state in Cu grains highly complex. The second requirement for forming five-fold twins and other multiple twins, *i.e.*, variation in stress orientation, is substantially met in the NMFs by partials emission from both interfaces and grain boundaries. As a result, multiple twins and even five-fold twins can be formed. Fig. 4(b) shows the intersection of two twins that are from interface and grain boundary, respectively. In the five-fold twin formed in present NMFs (Fig. 3(b)), strained planes adjacent to TB1, and TB3 are induced to accommodate the five-fold twin. The elastic strain is mainly produced by the internal lattice mismatch stress as mentioned above, which again demonstrate the characteristic of NMFs. For comparison, we show in Fig. 4(c) a TEM image of 60 nm-thick Cu thin film prepared by the same technologies, where only coplanar twins can be observed in the Cu grains with size ~50 nm. This further indicates that the formation of multiple twins as reported here is characteristic in NMFs.

A question come from the statistical results is why so many multiple twins are in the η = 9 multilayers, while much fewer in the η = 2 ones (Table 1). Two possible reasons are responsible for this difference. The first is related to the size-dependent "promotion-to-the next-layer" probability for twin formation [26]. The nucleation of one partial, while accounting for the stacking faults, is a necessary but not a sufficient condition for twins. Uncorrelated random emissions of individual partials cannot accidentally form a twin several of atomic layers thick, as those seen in Fig. 4(b). The emissions of partial dislocations, from both grain boundaries and interfaces, need to be spatially, and likely temporally, correlated. This layer-by-layer promotional effect may well be due to the inertia of a plane n partial dislocation, which can accumulate huge kinetic energy and move very fast after emission, driven by the high stress in grain interior, with total energy several times the stationary dislocation self-energy as it hits the grain boundary/interface, thus satisfying

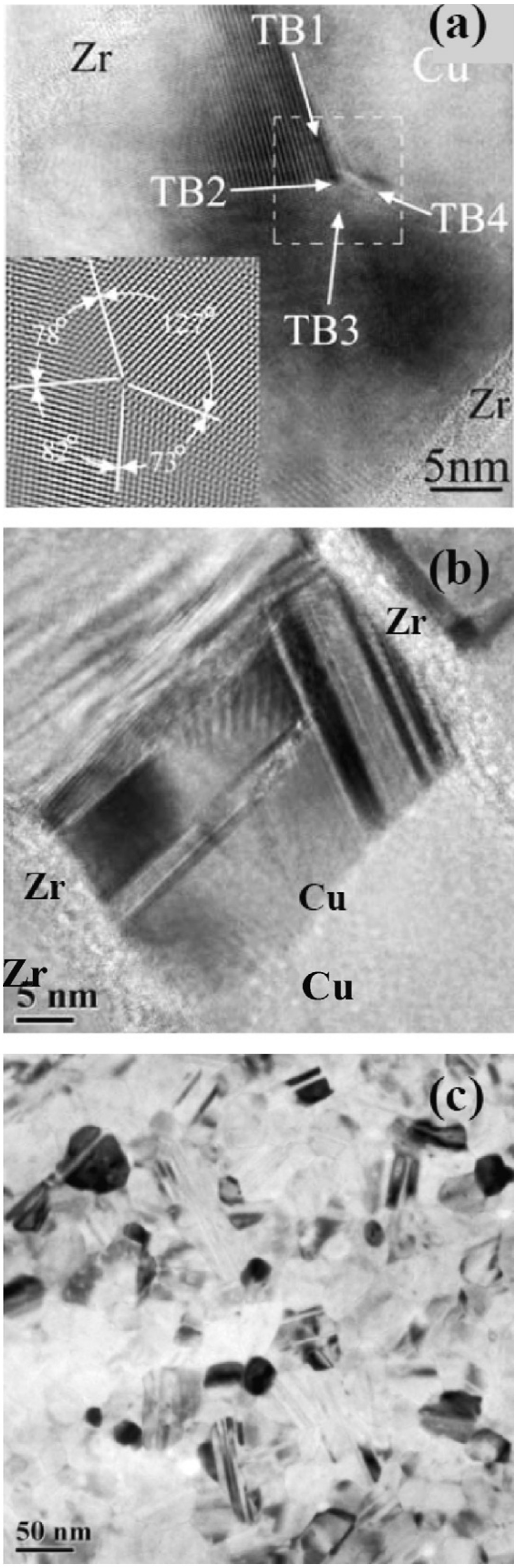

Fig. 4. (a) TEM image of a five-fold twin in the $\eta = 9$ NMFs, insert is the corresponding inverse fast Fourier transformation image; (b) TEM image displaying the intersection of two twins nucleated at interface and grain boundary, respectively; (c) TEM image of 60 nm-thick Cu single film showing the exclusive coplanar twins in grains, which is contrary to the multiple twins in Cu/Zr NMFs.

energy conservation for the creation of a partial dislocation on the plane $n+1$. The "promotion-to-the next-layer" probability is proportional to the grain size [26], *i.e.*, the smaller is the grain, the less is the probability for forming twins. The Cu grains in $\eta = 2$ NMFs, although having an in-plane size d_{Cu} close to those in $\eta = 9$ NMFs, are thinner in the out-of-plane direction (Table 1). The successive partial emission and resultantly twin formation from grain boundaries will be suppressed in the $\eta = 2$ NMFs. Fewer multiple twins are then formed in these multilayers compared to their $\eta = 9$ counterparts. The second possible reason is related to the grain shape-dependent stress gradient distribution in the Cu grains. For the Cu grains confined in layered structure, previous calculations [27] based on finite element methods showed that the difference in stress gradient between at interfaces and at grain boundaries is minimum, when the aspect ratio (A: the ratio between out-of-plane size and in-plane size) of the Cu grains is equal to 1. Under this condition, the partials can be readily emitted from both interfaces and grain boundaries. As the aspect ratio apart from 1, the difference between stress gradients at interfaces and at grain boundaries will be gradually broadened. Correspondingly, the partials will be preferentially emitted from either grain boundaries ($A > 1$) or interfaces ($A < 1$) and predominantly form single twins or coplanar twins. The Cu grains in $\eta = 9$ NMFs have an aspect ratio of about 1 (Table 1), indicating a more possibility of forming multiple twins than in $\eta = 2$ NMFs that have an aspect ratio of about 0.75.

3.3. Strengthening effect of multiple twins

Deformation mechanisms in NMFs have been extensively studied and some dislocation models have been suggested to account for the multilayer flow strength as a function of length scale from greater than a micrometer down to less than a nanometer [28–30]. When the layer thickness is only a few tens of nanometer, as in the case of present Cu/Zr NMFs, a confined layer slip (CLS) model can be used to well describe the increase in strength of the NMFs, which yield the following expression [30]

$$\sigma_{\text{cls}} = M\frac{\mu^* b}{8\pi h'}\left(\frac{4-\nu}{1-\nu}\right)\ln\left(\frac{\alpha h'}{b}\right) - \frac{F}{b} + \frac{\mu^*\varepsilon}{(1-\nu)} \tag{4}$$

where σ_{cls} is the stress required to propagate a glide loop of Burgers vector b confined to one softer Cu layer, M is the Taylor factor ($\sim$3), h' layer thickness parallel to the glide plane, ν is the Poisson ratio of Cu, $\mu^* = \mu_{Cu}\mu_{Zr}/2(V_{Zr}\mu_{Cu} + V_{Cu}\mu_{zr})$ is the mean shear modulus of Cu/Zr multilayers which can be estimated by the shear modulus μ_{Cu} and volume fraction V_{Cu} of the Cu layer and those of the Zr layer, the volume fraction of the Cu or Zr layer is directly related to the modulation ratio (*e.g.*, $V_{Cu} = \eta/(1+\eta)$), α represents the core cut-off parameter, F is the characteristic interface stress of multilayer, and the in-plane plastic strain ε is chosen as 1% here to calculate the flow strength [30]. With the parameters [30–32] of $\mu_{Cu} = 48.3$ GPa, $\mu_{Zr} = 32.8$ GPa, $\nu = 0.343$, $b = 0.2556$ nm, $\alpha = 1$, and $h' = h = 50\eta/(1+\eta)$ nm, the dependence of yield strength on interface stress F as a function of η is quantitatively calculated, as shown in Fig. 5. Yield strength is found to be insensitive to F within the range of $F = 2$–$4\,\text{J/m}^2$, but remarkably dependent on η, *i.e.*, the smaller is η and the higher is yield strength. This trend agrees well with general observation that smaller is stronger. When turn to the experimental results, however, it is surprising that the $\eta = 9$ Cu/Zr NMFs exhibit hardness or flow stress greater than the $\eta = 2$ NMFs, distinct from predicted trend. Since no other obvious differences existed between the two NMFs, such as in surface morphology, residual stress, and interface conditions, this discrepancy can be only explained by the difference in twins. Multiple twins is responsible for the higher hardness of the $\eta = 9$ Cu/Zr NMFs, and the single twins in $\eta = 2$ Cu/Zr NMFs make much less contribution to hardness. The significant strengthening effect caused by multiple twins can

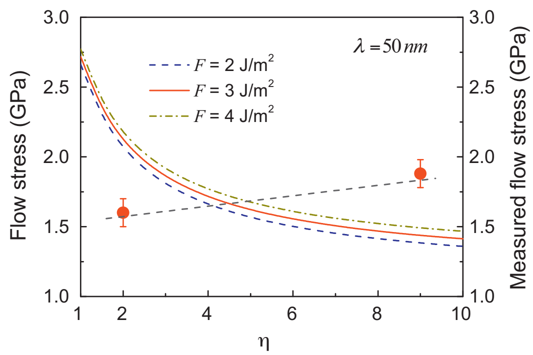

Fig. 5. Calculated dependence of flow stress on interface stress (F) as a function of η, showing the decrease in flow stress with increasing η. The Measured flow stresses (1/3 of the measured hardness) are also plotted in the figure (dots) to show a η-dependence distinct from calculations.

be understood as follows. Firstly, the multiple twins, especially the four-fold and five-fold twins, can impede the dislocation activity from various directions, which is impossible for the single twins. Secondly, the formation of multiple twins is accompanied with the partial relaxation of internal stress at both interfaces and grain boundaries, it will be hard to further emit partials. While in the case of single twins formed from interfaces (or grain boundaries), the partials can be easily emitted from the still-stressed other source of grain boundaries (or interfaces).

Here, we should mention that the NMFs used in previous investigations were usually kept η as constant of 1 and changed the modulation structure only in λ, where the interface effect was predominant over other strengthening factors. In present work, λ or interface density is unchanged and the interface strengthening is certain, the strengthening effect of multiple twins can be outstood.

4. Conclusions

A large number of multiple twins are experimentally observed in Cu/Zr NMFs with $\eta = 9$. The formation of multiple twins, especially four-fold and five-fold twins, is confirmed to occur through the sequential emission of partial dislocations from both interfaces and grain boundaries, driven by extremely high lattice mismatch stress and highly inhomogeneous microstructure that are characteristics of NMFs. The Cu/Zr NMFs with multiple twins have hardness greater than those with single twins, which indicates a significant strengthening effect of multiple twins.

Acknowledgments

This work was supported by the 973 Program of China (grant no. 2010CB631003), the 111 Project of China (B06025) and the National Natural Science Foundation of China (50971097). GL thanks the support of Fundamental Research Funds for the Central Universities and GJZ thanks the support of the Program for New Century Excellent Talents in University (grant no. NCET-10-0876).

References

[1] L. Lu, Y.F. Shen, X.H. Chen, L.H. Qian, K. Lu, Science 304 (2004) 422.
[2] E. Ma, Y.M. Wang, Q.H. Lu, M.L. Sui, L. Lu, K. Lu, Appl. Phys. Lett. 85 (2004) 4932.
[3] K. Lu, L. Lu, S. Suresh, Science 324 (2009) 349.
[4] X.Y. Li, Y.J. Wei, L. Lu, K. Lu, H.J. Gao, Nature 464 (2010) 877.
[5] T. Zhu, J. Li, A. Samanta, H.G. Kim, S. Suresh, Proc. Natl. Acad. Sci. U.S.A. 104 (2007) 3031.
[6] L. Lu, X. Chen, X. Huang, K. Lu, Science 323 (2009) 607.
[7] X. Zhang, O. Anderoglu, A. Misra, H. Wang, Appl. Phys. Lett. 90 (2007) 153101.
[8] X. Zhang, O. Anderoglu, R.G. Hoagland, A. Misra, JOM 60 (2008) 75.
[9] Y.T. Zhu, J. Narayan, J.P. Hirth, S. Mahajan, X.L. Wu, X.Z. Liao, Acta Mater. 57 (2010) 3763.
[10] X.L. Wu, Y.T. Zhu, Phys. Rev. Lett. 101 (2008) 025503.
[11] X.Z. Liao, Y.H. Zhao, Y.T. Zhu, R.Z. Valiev, D.V. Gunderov, J. Appl. Phys. 96 (2004) 636.
[12] X.Z. Liao, Y.H. Zhao, S.G. Srinivasan, Y.T. Zhu, R.Z. Valiev, D.V. Gunderov, Appl. Phys. Lett. 84 (2004) 592.
[13] X.L. Wu, J. Narayan, Y.T. Zhu, Appl. Phys. Lett. 93 (2008) 031910.
[14] Y.T. Zhu, X.Z. Liao, X.L. Wu, JOM 60 (2008) 60.
[15] P. Goudeau, K.F. Badawi, A. Naudon, G. Gladyszewski, Appl. Phys. Lett. 62 (1993) 246.
[16] B. Girault, P. Villain, E. Le Bourhis, P. Goudeau, P.O. Renault, Surf. Coat. Technol. 201 (2006) 4372.
[17] Y.T. Zhu, X.Z. Liao, R.Z. Valiev, Appl. Phys. Lett. 86 (2005) 103112.
[18] X.H. An, Q.Y. Lin, S.D. Wu, Z.F. Zhang, R.B. Figueiredo, N. Gao, T.G. Langdon, Scripta Mater. 64 (2011) 249.
[19] A.J. Cao, Y.G. Wei, Appl. Phys. Lett. 89 (2006) 041919.
[20] E.M. Bringa, D. Farkas, A. Caro, Y.M. Wang, J. McNancy, R. Smith, Scripta Mater. 59 (2008) 1267.
[21] J.Y. Huang, Y.K. Wu, H.Q. Ye, Acta Mater. 44 (1996) 1211.
[22] L.B. Freund, S. Suresh, Thin Film Materials: Stress, Defect formation and Surface Evolution, Cambridge University Press, Cambridge, 2003.
[23] M. Pletea, W. Brückner, H. Wendrock, J. Thomas, R. Kaltofen, R. Koch, J. Appl. Phys. 101 (2007) 073511.
[24] M.W. Chen, E. Ma, K.J. Hemker, H.W. Sheng, Y.M. Wang, X.M. Cheng, Science 300 (2003) 1275.
[25] S. Qu, X.H. An, H.J. Yang, C.X. Huang, G. Yang, Q.S. Zang, Z.G. Wang, S.D. Wu, Z.F. Zhang, Acta Mater. 57 (2009) 1586.
[26] J.Y. Zhang, G. Liu, R.H. Wang, J. Li, J. Sun, E. Ma, Phys. Rev. B 81 (2010) 172104.
[27] J. Zhang, J.Y. Zhang, G. Liu, Y. Zhao, J. Sun, Thin Solid Films 517 (2009) 2936.
[28] H.B. Huang, F. Spaepen, Acta Mater. 48 (2000) 3261.
[29] W.D. Nix, Metall. Mater. Trans. 20A (1989) 2217.
[30] A. Misra, J.P. Hirth, R.G. Hoagland, Acta Mater. 53 (2005) 4817.
[31] J.Y. Zhang, X. Zhang, G. Liu, G.J. Zhang, J. Sun, Scripta Mater. 63 (2010) 101.
[32] M.P. Puls, Metall. Mater. Trans. 21A (1990) 2905.